Origins of fractional control in regulated cell death

Luís C. Santos[1,+], Robert Vogel[2,1,+], Jerry E. Chipuk[4],
Marc R. Birtwistle[3,5,*], Gustavo Stolovitzky[2,1,*], and Pablo Meyer[2,1,*]

[1] Department of Genetics and Genomic Sciences, Icahn School of Medicine at Mount Sinai
New York, NY 10029, USA
[2] IBM T.J. Watson Research Center
Yorktown Heights, NY 10598, USA
[3] Systems Biology Center New York, Icahn School of Medicine at Mount Sinai
New York, NY 10029, USA
[4] Department of Oncological Sciences, Icahn School of Medicine at Mount Sinai
New York, NY 10029, USA
[5] Department of Chemical and Biomolecular Engineering, Clemson University
Clemson, SC 29634, USA
[+] These authors contributed equally
[*] To whom correspondence should be addressed;
Email: mbirtwi@clemson.edu, gustavo@us.ibm.com, pmeyerr@us.ibm.com

One Sentence Summary: Variable mitochondria abundance is a source of cell-to-cell variability that determines the fractional response of cells during regulated apoptosis.

Individual cells in clonal populations often respond differently to changes in environmental conditions; for binary phenotypes, such as cell death, this can be measured as a fractional response. These type of responses have been attributed to cell-intrinsic stochastic processes and variable abundances of biochemical constituents, such as proteins but the influence of organelles has yet to be determined. We use the response to TNF-related apoptosis inducing ligand

(TRAIL) and a new general method for quantifying heterogeneous responses to demonstrate that variable mitochondria abundance is a source of cell-to-cell variability that correlates with cell survival and determines the fractional cell death response. By quantitative data analysis, modeling and single cell experiments we attribute this effect to variable concentrations of the pro-apoptotic protein Bax on the mitochondrial surface. Further, we demonstrate that inhibitors of anti-apoptotic Bcl-2 family proteins, used in cancer treatment, may increase the diversity of cellular responses, enhancing resistance to the treatment.

Isogenic populations of cells in homogenous environments have the seemingly paradoxical capacity to generate many unique cell states. This ability is found in many, if not all single cell organisms and in the distinct cell types comprising multicellular organisms, as exemplified in the transient competent state of the bacterium *B. subtilis* (*1*), the differentiation of hematopoietic progenitor cells to either the erythroid or myeloid lineages (*2*), and in maintaining subpopulations in cancer (*3*). In all such cases, a cell's propensity for a particular state is attributed to the intrinsic stochasticity of low-copy number biomolecular reactions (*4–6*), or extrinsic variations in the abundances of its components (*7–9*). Taken together, they represent the so-called non-genetic sources of cell-to-cell variability (CCV).

One commonly studied source of CCV is protein abundance. Its premier status as a source of non-genetic CCV is due to its stochastic production (*6, 10*), and the sensitivity of cellular decision making machinery, e.g. signal transduction pathways, to the abundances of transcription factors, receptors, and/or enzymes (*11–14*). While it has been definitively shown that CCV in protein abundance influences cellular decisions, little attention has been given to other non-genetic sources of CCV.

There are numerous examples in which non-genetic and non-protein sources of CCV are

conjectured to impact biological phenomena. For example, centrosome abundance (*15*), the size of the Golgi apparatus (*16*), and mitochondria abundance (*17–19*) all have been shown to vary from cell-to-cell. Complementary to these observations, are measurements of the time to TRAIL-induced cell death of individual sister HeLa cells concomitantly treated with a potent inhibitor of protein translation, cyclohexamide, that became less correlated with time (*12, 20*). The origin of this decorrelation is unlikely to come from temporal fluctuations in protein abundance, but could originate from fluctuations in *organelle* abundances.

To determine if diversity in cell behaviors may be attributed to CCV in organelle abundance, we studied the role of mitochondria in the context of TRAIL induced apoptosis. TRAIL stimulates cell death by binding to its cognate death receptors on the cell surface forming a complex that activates Caspase 8, the so-called initiator caspase (IC). Active IC in turn causes Bax accumulation and multimerization on the outer membrane of mitochondria, forming pores (*21, 22*) which allow for the diffusion of pro-apoptotic molecules from the intermembrane space of the mitochondria into the cytosol (*23, 24*). These molecules activate a cascade which ultimately induces the activity of Caspase 3, the so-called executioner (EC) caspase (*23, 24*), which is responsible for triggering cell death. In effect, these molecules dynamically regulate each other's activity so that the continuous values of TRAIL concentration can be converted to a binary dead-or-alive response.

As found in many biological systems (*25, 26*), the conversion of a continuous input to a binary response limits the influence of CCV in cellular components to CCV in sensitivities. In apoptosis, each cell, with its unique concentrations of molecular components, requires a specific concentration of TRAIL that makes the cell die. At the population level the diversity in single-cell sensitivities to TRAIL gives rise to the fractional control of cell death. For example, consider an ensemble of cells with near identical biomolecular composition, or low CCV. With all components near equal, the individuals will undergo the life-death transition at nearly the

same dose of ligand (Fig.1A). In contrast, when CCV is relatively high, the individual cells of the ensemble will transition from live to dead at diverse doses of TRAIL (Fig.1B). The resulting fractional control of the population response to TRAIL would then take a steep or gradual sigmoidal shape, respectively.

From this interpretation, the empirical sigmoidal dose response curve represents the cumulative distribution of single-cell sensitivities. If we use the canonical Hill function to model the dose response curve, its parameters will be related to the moments of the probability density of single-cell sensitivities. Indeed, it can be shown that the half-max constant, IC_{50}, is equal to the mean and the Hill coefficient, n, is inversely proportional to the standard deviation of single-cell sensitivities (Fig. 1C) (see Supplementary Materials for derivation). Applying these statistical results provides a framework to quantitatively dissect sources of CCV and their influence on binary cellular response.

We apply this new statistical framework to quantitatively dissect sources of CCV and their influence on binary cellular response, using single-cell flow cytometry measurements (FCM) of mitochondria and their live-dead state in two cell lines: human T-lymphoblastoid derived cells (Jurkat) and a human breast adenocarcinoma cell line (MDA-MB-231). These cells were exposed to different doses of TRAIL for four hours, a timeframe in which cells died but the single cell abundances of mitochondria per unit cell size, density ρ (Fig. S1), remained largely unchanged (Fig. S2). The single-cell FCM were then used to identify living cells (Fig. 2A and Fig. S3) and to characterize the fractional response of the population to TRAIL (Fig. 2B inset). Using our statistical interpretation of the Hill model, we find that the IC_{50}, and consequently the mean sensitivity, to be 3.81 ± 0.26 ng/mL and 76.4 ± 8.77 ng/mL in Jurkat and MDA-MB-231 cells, respectively. The variance of single-cell sensitivities to TRAIL is 1.5 fold higher in Jurkat than it is in MDA-MB-231.

In conjunction with the fractional response to TRAIL, the distribution of mitochondria den-

sity among living cells became increasingly enriched for cells with higher ρ with increasing TRAIL dose (Fig. 2B). We hypothesized that the observed enrichment is established by a differential sensitivity of single-cells to TRAIL based upon their mitochondria density. We tested this hypothesis quantitatively by means of Bayes' theorem, which allows us to estimate the conditional probability that a cell is alive given ρ for each dose of TRAIL (Fig. 2C-D, Fig.S4 and Supplementary Materials for derivation). Application to experimental measurements in Jurkat cells shows that the changes in the mitochondria density distribution in Fig. 2B is quantitatively associated with the fractional response to TRAIL (Fig. 2C and Fig.S5). Using this finding, we extended our investigation to assessing the influence of mitochondria on the fractional response of single-cells (Fig. 2D). The $IC_{50}(\rho)$ of TRAIL positively scales with mitochondria density (Fig. 2E) in Jurkat cells. In contrast, in MDA-MB-231 cells the $IC_{50}(\rho)$ of TRAIL was less dependent on mitochondria density. Quantitatively, 30% and 2% of the diversity in single-cell sensitivities to TRAIL may be attributed to mitochondria density in Jurkat and MDA-MB-231 cells, respectively (Fig. 2F, see Supplementary materials for derivation Fig. S6-11).

To gain mechanistic insight to the functional role of mitochondria density in the cell death decision, we developed a coarse-grained dynamic model of apoptosis. Our description aims to reproduce the dominant dynamical features of initiator caspase reporter protein (IC-RP) first measured and published by Albeck *et al.* (*23*). These being a slow but accelerating initial increase of IC followed by a fast increase in both IC and EC (see Fig. S12). To such end our model includes: i) a slow autocatalytic increase in IC activation, ii) a quasi-steady-state approximation for Bax pore formation dynamics and mitochondrial outer membrane permeabilization (MOMP), and iii) the strong positive feedback from EC to IC (Fig. 3A, see Supplementary materials for details).

We conjectured that TRAIL induced activation of IC in Jurkat and MDA-MB-231 cells match the biphasic increase of IC-RP measured in HeLa cells (*23*), but differ in their propensity

to form Bax pores (Fig. 3B-C). Specifically, we consider unique susceptibilities of Bax pore formation to Bcl-2 mediated inhibition for each cell line. As Bax pores reside in the mitochondria, the effective Bax concentration for a given amount of Bax decreases with mitochondria density. Implementing this insight into the model equations we see that the influence of mitochondria density can be understood through the corresponding bifurcation diagrams (Fig. 3D-E).

The dynamic properties of IC in MDA-MB-231 cells in the absence of TRAIL are either bistable or monostable depending on mitochondria density. In these diagrams, the high IC fixed point corresponds to cells that have integrated sufficient signal for MOMP and consequently represent apoptotic cells. According to Fig. 3D, cells with relatively low mitochondria density are bistable and may undergo apoptosis only if their IC abundance exceeds a critical amount designated by the dashed line. This bistable region does not preclude cell death - cells may acquire sufficient abundances of IC for death by fluctuations in biomolecular reactions. Indeed, the likelihood of such an event decreases with the difference of IC abundance between the unstable fixed point (dashed line) and low IC stable fixed point (solid line). Meanwhile, cells with relatively high mitochondria density only have a single fixed point of low IC, indicating that these cells will never spontaneously undergo apoptosis in the absence of TRAIL.

In contrast, the bifurcation diagram representing Jurkat cells shows three distinct regions (Fig. 3E). These being cells with: 1) low density of mitochondria having a single fixed point of high IC and consequently all die; 2) medium density of mitochondria are bistable, for which, the fractional response to TRAIL decreases with the concomitant increase in the IC unstable fixed point and mitochondria density; and 3) high density of mitochondria are monostable with low IC abundances, hence all cells survive. Next, we extend these analyses to the full range of TRAIL doses.

The influence of increasing TRAIL dose in each cell type specific parameterized model is evident in their bifurcation diagrams. MDA-MB-231 cells respond to TRAIL by increasing the

IC abundance of the lower fixed point (Fig. 3F). In doing so, cells with mitochondria density in the bistable region equally increase their susceptibility to cell death from fluctuations in IC abundance. The Jurkat models response to TRAIL exhibits an increase of the density of mitochondria that separates the monostable high and bistable IC abundance regions (Fig. 3G). Therefore, an individual cell's mitochondria density determines its sensitivity to TRAIL induced cell death. Together, these model-based observations propose an explanation for how CCV in mitochondria density influences the response of Jurkat but to a lesser extent MDA-MB-231 cells to TRAIL.

In inspecting the model parameters associated with each cell type, we noticed that MDA-MB-231 cells were more susceptible to Bcl-2 mediated inhibition of Bax pore formation than Jurkat. We hypothesized that this effect would be abated by incorporating a small molecule inhibitor to Bcl-2 in MDA-MB-231 cells (Fig. 4A see Supplementary materials for derivation). By incorporating Bcl-2 inhibition, we found that the sensitivity of the fractional response of the cell population to TRAIL increases (Fig. 4B). Furthermore, and as intuited, Bcl-2 inhibition increased the dependence of single-cell sensitivities to TRAIL on mitochondria density (Fig. 4D). We corroborated these theoretical predictions by measuring the influence of the clinically relevant small molecule inhibitor of Bcl-2 family proteins ABT-263 (*27*) (Fig. 4C and E). Remarkably, Bcl-2 inhibition alone increased the variance of sensitivities attributable to mitochondria density from 0% to 40% (Fig. 4F).

Extending previous work that observed that mitochondria abundance differs among individual clonal cells without characterizing the role of this CCV in biological processes, we have unveiled a fundamental connection in the CCV of mitochondria to the fractional control of TRAIL induced cell death. Using mathematical modeling we attribute this connection to the dilution of Bax on the outer mitochondrial membrane in cells with higher densities of mitochondria. From these quantitative insights, we found that the functional manifestation of mitochondrial CCV is

plastic - readily and predictably tunable by small molecule inhibitors of Bcl-2. It is plausible that this plasticity is a tool accessible to cells, and therefore may be co-opted by pathological cellular populations. For example, high mitochondria abundance can be a non-genetic mechanism of resistance to pro-apoptotic therapeutics. Incorporation of such knowledge may be an important consideration in developing therapeutic strategies. Furthermore, such an advantage may manifest in time-scales much longer than the life span of a single cell or the disease in a human, but propagate to the long time-scales of evolution. To date, the evolutionary hypothesis of mitochondria is as a symbiotic bacterium inside a proto-eukaryotic cell (*28*), exchanging safety for energy. However, another such evolutionary advantage may be expected, that this symbiosis would create a survival advantage such as the one described here. These results suggest that environmental constraints can select subpopulations not only based on genetic composition, protein abundances, but also CCV in organelle abundances.

References and Notes

1. G. M. Süel, J. Garcia-Ojalvo, L. M. Liberman, M. B. Elowitz, *Nature* **440**, 545 (2006).

2. H. Chang, M. Hemberg, M. Barahona, D. Ingber, S. Huang, *Nature* **453** (2008).

3. P. B. Gupta, *et al.*, *Cell* **146**, 633 (2011).

4. M. B. Elowitz, A. J. Levine, E. D. Siggia, P. S. Swain, *Science* **297**, 1183 (2002).

5. J. M. Pedraza, A. van Oudenaarden, *Science* **307**, 1965 (2005).

6. L. Cai, N. Friedman, X. S. Xie, *Nature* **440** (2006).

7. A. Raj, A. van Oudenaarden, *Cell* **135**, 216 (2008).

8. A. Eldar, M. B. Elowitz, *Nature* **467**, 167 (2010).

9. G. Balázsi, A. van Oudenaarden, J. J. Collins, *Cell* **144**, 910 (2011).

10. N. Friedman, L. Cai, X. S. Xie, *Phys. Rev. Lett.* **97**, 168302 (2006).

11. O. Feinerman, J. Veiga, J. R. Dorfman, R. N. Germain, G. Altan-Bonnet, *Science* **321**, 1081 (2008).

12. S. Spencer, S. Gaudet, J. Albeck, J. Burke, P. Sorger, *Nature* **459** (2009).

13. J. W. Cotari, G. Voisinne, O. E. Dar, V. Karabacak, G. Altan-Bonnet, *Sci. Signal.* **6**, ra17 (2013).

14. R. M. Vogel, A. Erez, G. Altan-Bonnet, *Nature Communications* p. 12428 (2016).

15. B. R. Brinkley, *Trends in Cell Biology* **11**, 18 (2001).

16. Y. Guo, A. D. Linstedt, *The Journal of Cell Biology* **174**, 53 (2006).

17. E. D. Robin, R. Wong, *Journal of Cellular Physiology* **136**, 507 (1988).

18. R. P. das Neves, *et al.*, *PLOS Biology* **8**, 1 (2010).

19. I. G. Johnston, *et al.*, *PLOS Computational Biology* **8**, 1 (2012).

20. The study by Spencer *et al.* (*12*) compared the correlation time-scale of sister HeLa cells' time to TRAIL induced cell death in the presence and absence of cyclohexamide. From which, they found that temporal fluctuations in protein abundance do contribute to CCV in time to death. An interpretation we do not disagree with, however these same data also suggests that protein is not the only contributing factor.

21. W.-X. Zong, T. Lindsten, A. J. Ross, G. R. MacGregor, C. B. Thompson, *Genes & Development* **15**, 1481 (2001).

22. M. C. Wei, *et al.*, *Science* **292**, 727 (2001).

23. J. G. Albeck, *et al.*, *Molecular Cell* **30**, 11 (2008).

24. J. G. Albeck, J. M. Burke, S. L. Spencer, D. A. Lauffenburger, P. K. Sorger, *PLOS Biology* **6**, 1 (2008).

25. J. E. Ferrell, E. M. Machleder, *Science* **280**, 895 (1998).

26. S. Tay, *et al.*, *Nature* **466**, 267 (2010).

27. C. Tse, *et al.*, *Cancer Research* **68**, 3421 (2008).

28. L. Margulis, *Symbiosis in cell evolution: Life and its environment on the early earth* (Freeman, San Francisco, 1981).

29. MDA-MB-231 experiments were performed in triplicate, one data set showed effectively zero scaling and hence the x-axis parameter is undefined, consult the Supplementary materials to examine the raw data.

Acknowledgments

This research was funded in part by grants from the NIH, (P50GM071558 (Systems Biology Center New York), R01GM104184 and U54HG008098 (LINCS Center) for MRB, R01 CA206005 for J.E.C. and P30 CA196521 a Tisch Cancer Institute Cancer Center Support Grant) and also an IBM faculty award for MRB. We wish to thank John Albeck for sharing single cell data and staff of the flow cytometry core facility at ISMMS and Julia Moore Vogel for help with the manuscript. Author Contributions: All authors together interpreted the results, approved the design of the figures and the text, which were prepared by R.V., L.S., G.S., M.R.B. and P.M.

Supplementary Materials

Materials and Methods

Table S1 and S2

Fig S1 to S12

References (30-39)

Fig. 1. Cell-to-cell variability in the binary response to TRAIL. A Hill function response curve (blue) to TRAIL dose (x-axis in log scale) and the corresponding probability density of the single-cell sensitivities (orange) for populations with (A) low CCV and (B) high CCV. (C) The correspondence between the variance of single-cell sensitivities (σ) to TRAIL and the Hill coefficient n. Here, (n_A, σ_A) and (n_B, σ_B) represent the Hill coefficient and corresponding single-cell variances from (A) and (B), respectively.

Fig. 2. CCV in mitochondrial density influences fractional response to TRAIL. (A) Flow cytometry measurements (FCM) of mitochondria (MitoTracker Deep Red) and phosphatidylserine (FITC conjugated Annexin V) per Jurkat cell. (B) The probability density of mitochondrial density (ρ) and fractional response of Jurkat cells to TRAIL (inset). Each color corresponds to a specific dose of TRAIL. (C) The inferred Hill function representing the probability that a Jurkat cells is alive at a given mitochondria density for different TRAIL doses. (D) The inferred Hill function representing the probability that a Jurkat cell is alive given TRAIL dose and for a given mitochondria density. (E) The dose of TRAIL normalized to the population $\langle \mathrm{IC}_{50} \rangle$ (y-axis) and the inferred density of mitochondria (ρ) in which the probability of survival is 0.5 (x-axis). Markers designate Jurkat (blue) triplicate averages and MDA-MB-231 (orange) triplicate averages of $\mathrm{IC}_{50}(\rho)/\langle \mathrm{IC}_{50} \rangle$ but duplicate ρ (*29*), error bars are the respective standard error of the mean, while dotted lines represent individual experiments. (F) The fraction of the variance in single cell TRAIL sensitivities (σ) explained by CCV in mitochondria density from E (σ_ρ).

Fig. 3. Mechanism of IC_{50} dependence on mitochondria density. (A) Simple model of apoptosis. The dynamics of initiator caspase reporter protein (IC-RP) from (*23*) and the model-inferred dynamics corresponding to (B) MDA-MB-231 and (C) Jurkat cell lines. The model bifurcation diagrams for [TRAIL] = 0 ng/mL in (D) MDA-MB-231 and (E) Jurkat cells. The influence of TRAIL dose on the model fixed points for (F) MDA-MB-231 and (G) Jurkat cells.

The dependence of single cell sensitivities to TRAIL on ρ for (H) MDA-MB-231 and (I) Jurkat cells. The IC_{50} was estimated from Hill function fits of simulated data (blue circles), and which were then fit to a power law (black line). Simulations consisted of 100 cells per each of the 20 doses of TRAIL and 12 densities of mitochondria considered.

Fig. 4. Plasticity in fractional response to TRAIL. (A) Bcl-2 inhibitor reduces the effective abundance of Bcl-2 by formation of Bcl-2:Bcl-2 inhibitor complex. (B) Simulation results of the population $IC_{50}{}^{\mathrm{TRAIL}}$ response to Bcl-2 inhibition in MDA-MB-231 cells. (C) Experimental measurement sets (markers) of the population $IC_{50}{}^{\mathrm{TRAIL}}$ response to Bcl-2 inhibition for MDA-MB-231 cells. (D) Estimated IC_{50} for changing ρ from MDA-MB-231 parameterized model simulations. (E) The experimental dependence of IC_{50} on ρ, as computed in Fig. 2E, for [0, 1, 3, 10] μM doses of the Bcl-2 Inhibitor ABT-263. (F) The fraction of variance in single-cell sensitivities (σ) explained by mitochondria density CCV in E (σ_ρ). Note that all simulations were conducted with 100 cells for each 20 doses of TRAIL, 12 densities of log-normally distributed mitochondria, and 9 doses of inhibitor.

Figure 1

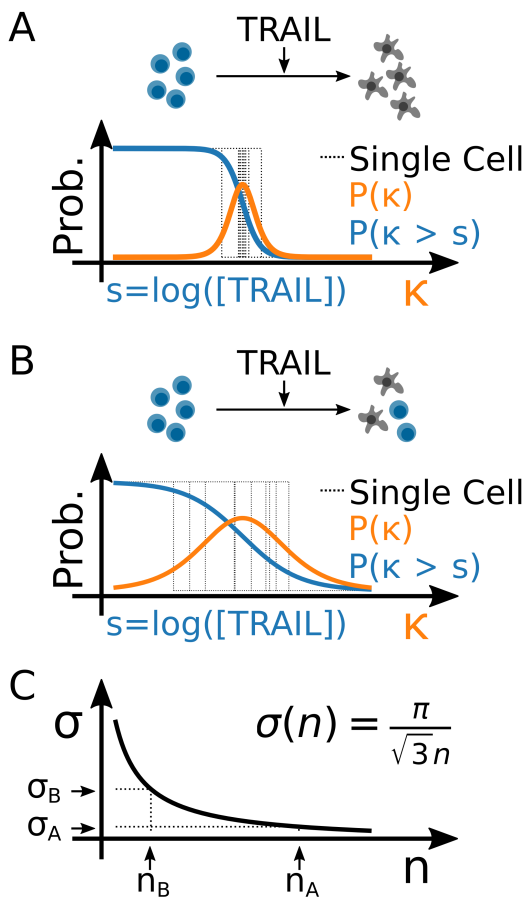
A
TRAIL
Single Cell
P(κ)
P(κ > s)
Prob.
s=log([TRAIL])
κ
B
TRAIL
Single Cell
P(κ)
P(κ > s)
Prob.
s=log([TRAIL])
κ
C
σ
$\sigma(n) = \frac{\pi}{\sqrt{3}n}$
σ_B
σ_A
n_B
n_A
n

Figure 2

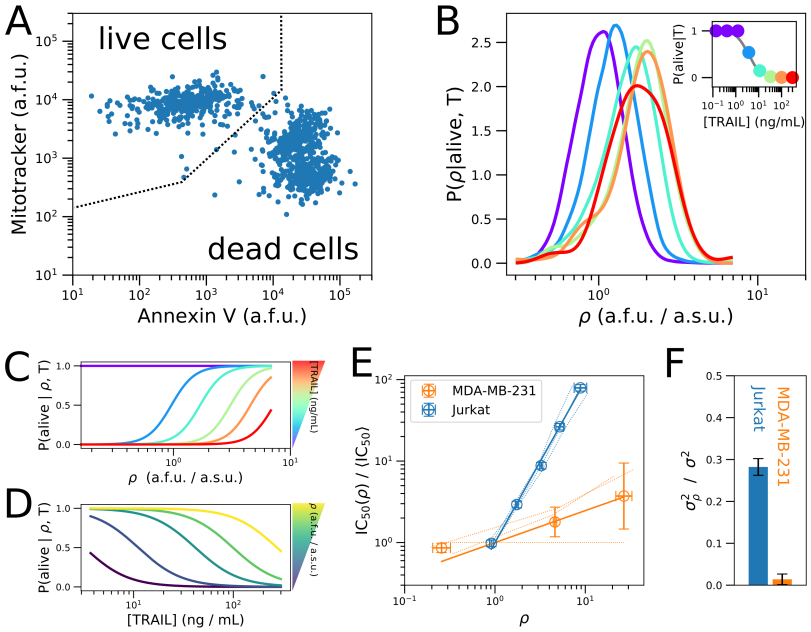
A
live cells
dead cells
Mitotracker (a.f.u.)
Annexin V (a.f.u.)
B
P(ρ|alive, T)
ρ (a.f.u. / a.s.u.)
P(alive|T)
[TRAIL] (ng/mL)
C
P(alive | ρ, T)
ρ (a.f.u. / a.s.u.)
[TRAIL] (ng/mL)
D
P(alive | ρ, T)
[TRAIL] (ng / mL)
ρ (a.f.u. / a.s.u.)
E
MDA-MB-231
Jurkat
IC50(ρ) / (IC50)
ρ
F
Jurkat
MDA-MB-231
σ²ρ / σ²

Figure 3

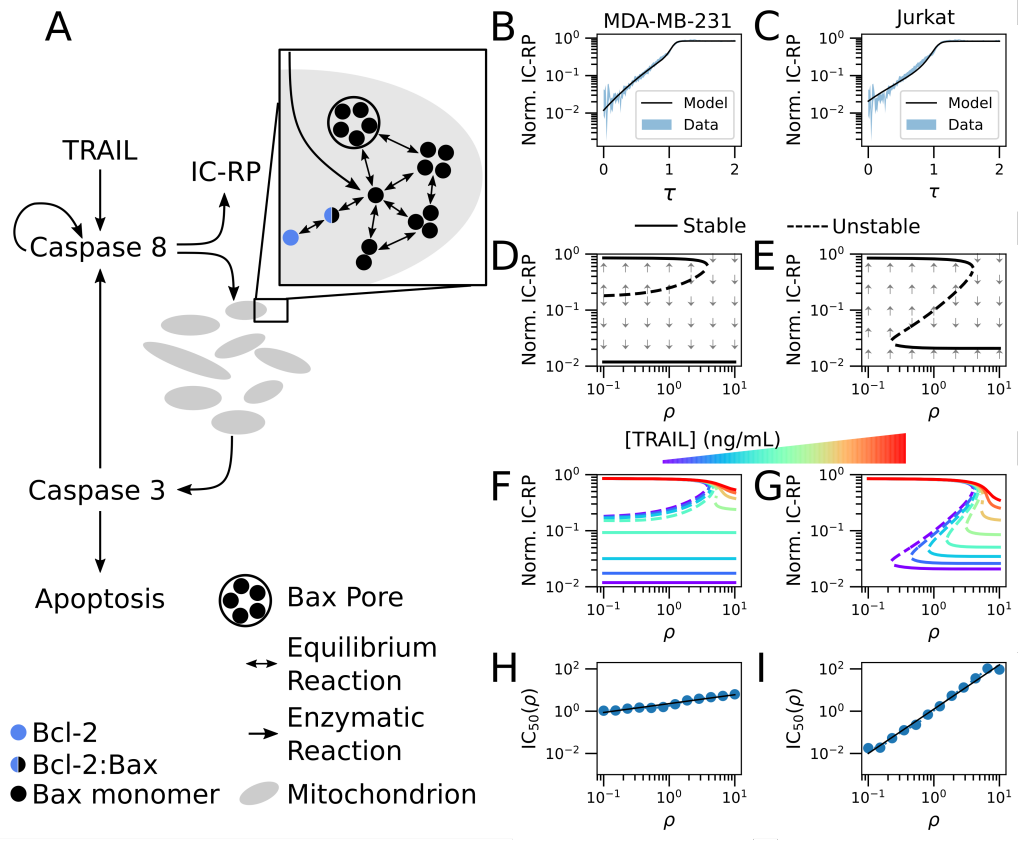
A
TRAIL
IC-RP
Caspase 8
Caspase 3
Apoptosis
Bax Pore
Equilibrium Reaction
Enzymatic Reaction
Mitochondrion
Bcl-2
Bcl-2:Bax
Bax monomer
B
MDA-MB-231
C
Jurkat
Norm. IC-RP
Model
Data
τ
Stable
Unstable
D
E
ρ
[TRAIL] (ng/mL)
F
G
H
I
IC50(ρ)

Figure 4

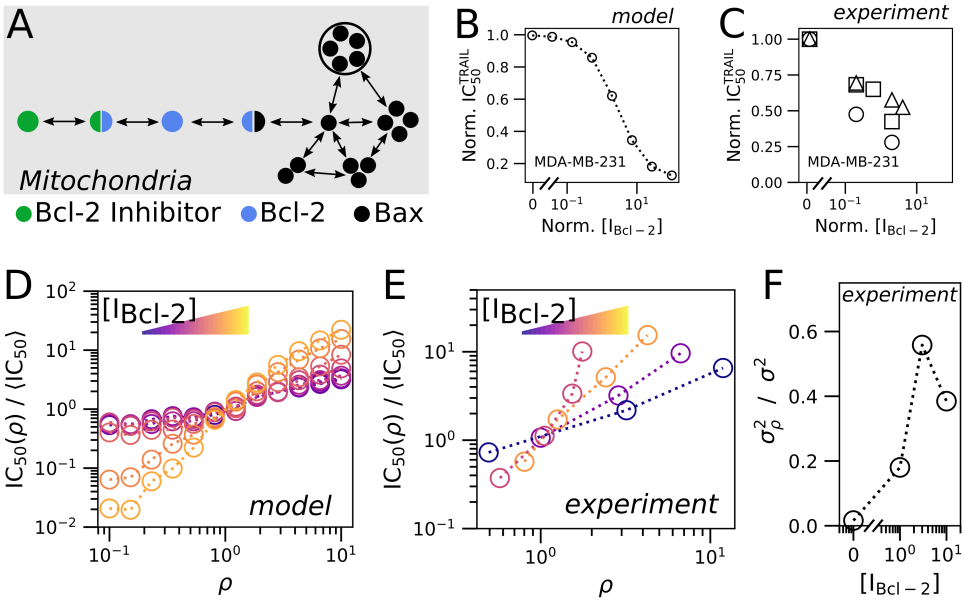
A
Mitochondria
Bcl-2 Inhibitor
Bcl-2
Bax
B
model
Norm. IC_{50}^{TRAIL}
MDA-MB-231
Norm. $[I_{Bcl-2}]$
C
experiment
Norm. IC_{50}^{TRAIL}
MDA-MB-231
Norm. $[I_{Bcl-2}]$
D
$[I_{Bcl-2}]$
$IC_{50}(\rho) / \langle IC_{50} \rangle$
model
ρ
E
$[I_{Bcl-2}]$
$IC_{50}(\rho) / \langle IC_{50} \rangle$
experiment
ρ
F
experiment
σ_ρ^2 / σ^2
$[I_{Bcl-2}]$